30th International Conference
ENGINEERING MECHANICS 2024
Milovy, Czech Republic, May 14 – 16, 2024

INFLUENCE OF BERKOVICH INDENTER TILT ON THE PROJECTED CONTACT AREA AT NANOINDENTATION TEST

Kovář J.*, Fuis V.**

Abstract: *At the nanoindentation test, the tilt of the indenter or specimen surface can occur. This deviation influences the projected contact area, which is important for the evaluation of the Young modulus and hardness. This paper is aimed on the derivation of the analytical expressions for the projected contact area if the indenter is tilted in 3D space. Then the projected contact area is the same as the area of indenter cross-section by the plane corresponding to the specimen surface. The calculated results for tilted and ideal indenter were compared and the influence of the indenter tilt was evaluated. The cross-sections were plotted for few indenter tilts to better describe the change of the projected contact area. The results show that indenter tilt can have significant impact on the results if the indenter tilt is big enough.*

Keywords: Berkovich indenter, tilt, nanoindentation, projected contact area, shape function.

1. Introduction

The nanoindentation test is well-known method for determination of the Young modulus and hardness of the tested specimen (Oliver, 1992). To obtain correct results, the projected contact area to the specimen surface has to be known. This area is influenced by the indenter or the specimen tilt in 3D space. When the specimen is tilted, the projected contact area is the same as the area of indenter cross-section by a plane of specimen surface. The analytical expressions for the area of the sections of mostly used Berkovich indenter (Fig. 1), which has the shape of the three-sided pyramid, were already derived (Shi, 2013). However, simplifications, which could have influence to the calculated results, were used; therefore, derivation of expressions will be done without these simplifications in this paper to evaluate the influence of the specimen tilt on the projected contact area and results of nanoindentation more precisely.

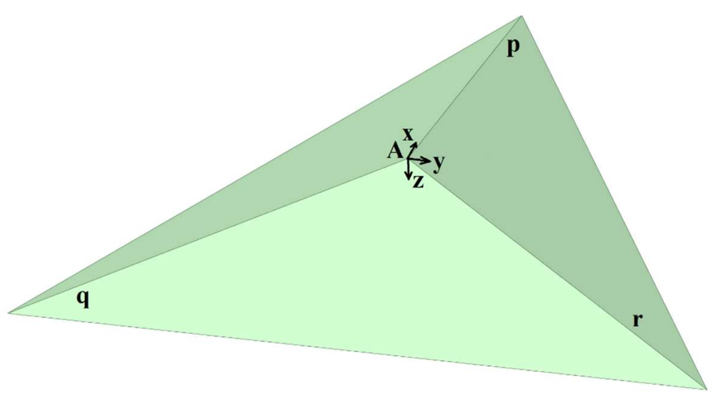

Fig. 1: Berkovich indenter.

* Ing. Jaroslav Kovář, PhD.: Institute of Solid Mechanics, Mechatronics and Biomechanics, Brno University of Technology, Technická 2896/2; 616 69, Brno; CZ, jaroslav.kovar@vut.cz

** Assoc. Prof. Ing. Vladimír Fuis, PhD.: Centre of Mechatronics – Institute of Thermomechanics of the Czech Academy of Sciences – branch Brno and Faculty of Mechanical Engineering, Brno University of Technology, Technická 2896/2; 619 69, Brno, CZ, fuis@it.cas.cz

doi: 10.21495/em2024-166

2. Derivation of the analytical expressions

The modified Berkovich indenter, here referred to as Berkovich indenter, is defined by only one parameter, which is the angle between the z-axis and the center of the side of the indenter at the section of the indenter (α in Fig. 2). The commonly used value of this parameter is $\alpha = 65.3\,°$ (Borodich, 2003). To make the following derivation more clear, the opposite angle (φ) was used. The relation between these parameters is given by (1).

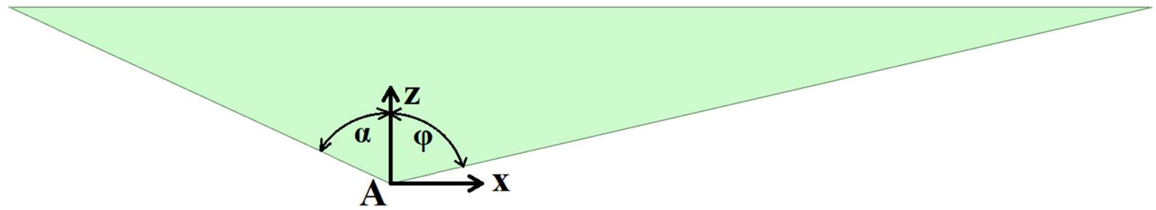

Fig. 2: Section of the Berkovich indenter by xz-plane.

$$\tan\varphi = 2 \cdot \tan\alpha \tag{1}$$

2.1. Parametrization of the indenter edges

If the indenter is cut by a plane, the cross-section is triangular, with the apexes at the intersection of the cutting plane with indenter edges. From the geometry of the indenter (Figs. 1 and 2), the unit vectors of indenter edges were derived and because all edges come out from the origin of the coordinate system (point A), the parametric equations of the edges can be expressed by (2) ÷ (4). The parameter can reach the infinity, because the indenter was expected as unbounded from the upper side.

$$p: \quad x = \frac{\tan\varphi \cdot p_1}{\sqrt{\tan^2\varphi + 1}}\,; \quad y = 0\,; \quad z = \frac{p_1}{\sqrt{\tan^2\varphi + 1}} \qquad p_1 \epsilon \langle 0; \infty) \tag{2}$$

$$q: \quad x = \frac{-\tan\varphi \cdot \sin 30° \cdot p_2}{\sqrt{\tan^2\varphi + 1}}\,; \quad y = \frac{\tan\varphi \cdot \cos 30° \cdot p_2}{\sqrt{\tan^2\varphi + 1}}\,; \quad z = \frac{p_2}{\sqrt{\tan^2\varphi + 1}} \qquad p_2 \epsilon \langle 0; \infty) \tag{3}$$

$$r: \quad x = \frac{-\tan\varphi \cdot \sin 30° \cdot p_3}{\sqrt{\tan^2\varphi + 1}}\,; \quad y = \frac{-\tan\varphi \cdot \cos 30° \cdot p_3}{\sqrt{\tan^2\varphi + 1}}\,; \quad z = \frac{p_3}{\sqrt{\tan^2\varphi + 1}} \qquad p_3 \epsilon \langle 0; \infty) \tag{4}$$

2.2. Parametrization of the section plane

The next step was the obtaining of the equation for the slice plane ρ. This plane was created from the plane *xy*, which was firstly rotated by angle ε around the *x*-axis, then about λ around *y*-axis and finally moved in the way of *z*-axis about the value of the contact depth (h_c) which is depending on the indentation depth (Oliver, 1992). For this plane, the unit vectors were derived and the normal vector was derived by its cross product (5). When the normal vector was known, the equation of the section plane (6) was derived.

$$\overrightarrow{n_\rho} = (\cos\varepsilon \cdot \sin\lambda\,; -\cos\lambda \cdot \sin\varepsilon\,; \cos\lambda \cdot \cos\varepsilon) \tag{5}$$

$$\rho: \quad \cos\varepsilon \cdot \sin\lambda \cdot x - \sin\varepsilon \cdot \cos\lambda \cdot y + \cos\varepsilon \cdot \cos\lambda \cdot z - \cos\varepsilon \cdot \cos\lambda \cdot h_c = 0 \tag{6}$$

2.3. Determination of the edges of cross-section

From the parametric equations of the edges (2 ÷ 4) and the equation of the plane (6), the coordinates of the apexes of the triangular cross-section were derived (7 ÷ 9) (B, C, and D in Fig. 3). These coordinates are dependent on the values of parameters from (2 ÷ 4), which can be determined in the intersection of the edges and plane according to (10 ÷ 12).

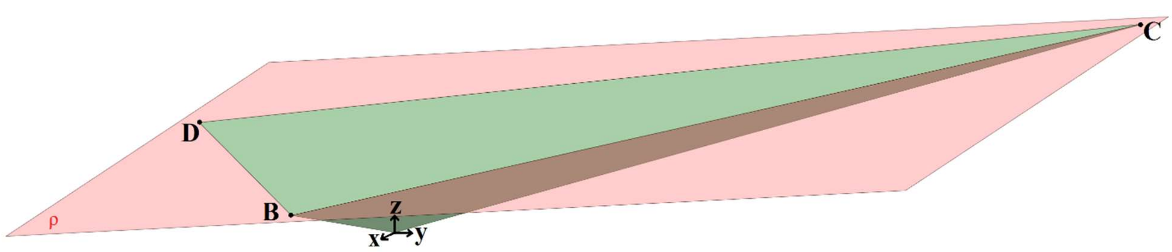

Fig. 3: Section of the Berkovich indenter by tilted plane.

$$B = \left[\frac{\tan\varphi \cdot p'_1}{\sqrt{\tan^2\varphi+1}}; 0; \frac{p'_1}{\sqrt{\tan^2\varphi+1}}\right] \tag{7}$$

$$C = \left[\frac{-\tan\varphi \cdot \sin 30° \cdot p'_2}{\sqrt{\tan^2\varphi+1}}; \frac{\tan\varphi \cdot \cos 30° \cdot p'_2}{\sqrt{\tan^2\varphi+1}}; \frac{p'_2}{\sqrt{\tan^2\varphi+1}}\right] \tag{8}$$

$$D = \left[\frac{-\tan\varphi \cdot \sin 30° \cdot p'_3}{\sqrt{\tan^2\varphi+1}}; \frac{-\tan\varphi \cdot \cos 30° \cdot p'_3}{\sqrt{\tan^2\varphi+1}}; \frac{p'_3}{\sqrt{\tan^2\varphi+1}}\right] \tag{9}$$

$$p'_1 = \frac{h_c \cdot \sqrt{\tan^2\varphi+1}}{\tan\lambda \cdot \tan\varphi+1} \tag{10}$$

$$p'_2 = \frac{h_c \cdot \sqrt{\tan^2\varphi+1}}{-\sin 30° \cdot \tan\lambda \cdot \tan\varphi - \cos 30° \cdot \tan\varepsilon \cdot \tan\varphi +} \tag{11}$$

$$p'_3 = \frac{h_c \cdot \sqrt{\tan^2\varphi+1}}{-\sin \quad ° \cdot \tan\lambda \cdot \tan\varphi + \cos 30° \cdot \tan\varepsilon \cdot \tan\varphi+1} \tag{12}$$

2.4. Derivation of the surface of cross-section

From the known apexes of the triangle (7–9), the area of the cross-section was calculated. The two vectors corresponding to the edges of the triangle were created and then the cross-section area was determined as the half of its cross product size. The resulting expression (13) was depended on the values p'_1, p'_2, and p'_3 (10–12). When these parameters were substituted to the (13), the final equation (14) was derived by Matlab with the relation between parameters φ and α from (1).

$$A_c = \frac{\sqrt{3} \cdot \tan\varphi}{4 \cdot (\tan^2\varphi+1)} \cdot \sqrt{(2 \cdot p'_2 \cdot p'_3 - p'_1 \cdot p'_2 - p'_1 \cdot p'_3)^2 + 3 \cdot (p'_1 \cdot p'_3 - p'_1 \cdot p'_2)^2 + \tan^2\varphi \cdot (p'_1 \cdot p'_2 + p'_2 \cdot p'_3 + p'_1 \cdot p'_3)^2} \tag{13}$$

$$A_c = 3^{\frac{3}{2}} \cdot h_c^2 \cdot \tan^2\alpha \cdot \sqrt{\frac{\tan^2\varepsilon+\tan^2\lambda+1}{(2 \cdot \tan\alpha \cdot \tan\lambda + \quad)^2 \cdot \left(2 \cdot \tan\alpha \cdot \tan\lambda - 1 + \tan^2\alpha \cdot (3 \cdot \tan^2\varepsilon - \tan^2\lambda)\right)^2}} \tag{14}$$

The cross-section for the untilted Berkovich indenter can be determined by (15) (Oliver, 1992). Then the ratio between the cross-sectional areas of the tilted and untilted indenter can by determined by (16). Ratio is dependent only on the angles of tilt (ε and λ) and the indenter angle α.

$$A_{c0} = 3^{\frac{3}{2}} \cdot h_c^2 \cdot \tan^2\alpha \tag{15}$$

$$\frac{A_c}{A_{c0}} = \sqrt{\frac{\tan^2\varepsilon+\tan^2\lambda+1}{(2 \cdot \tan\alpha \cdot \tan\lambda+1)^2 \cdot \left(2 \cdot \tan\alpha \cdot \tan\lambda - 1 + \tan^2\alpha \cdot (3 \cdot \tan^2\varepsilon - \tan^2\lambda)\right)^2}} \tag{16}$$

3. Results and discussion

The Berkovich indenter was cut by the plane at the indentation depth 100 nm, the section plane was tilted and the areas of cross-sections were calculated according to (14). The relative differences between the areas obtained by tilted and untilted section planes are shown in Fig. 4. The plotted surface shows that the difference is symmetrical for the positive and negative values of the tilt in *x*-axis. This is due to the same symmetry of the indenter. The calculated results show difference against the expression determined by (Shi, 2013), due to the simplifications which were used in their derivation. The Berkovich indenter was modelled in the 3D CAD software Autodesk Inventor and the areas of its cross-sections by tilted plane were measured and compared with the results of analytical calculations. Both methods gave the same values. To better depiction of the tilt influences, the tilted and untilted planes were plotted for few combinations of the angles ε and λ in Fig. 5. The values of angles were chosen according to Fig. 4. All calculations assumed tilted surface of the tested specimen (section plane), as the indenter is tilted, the contact depth needs to be corrected for the influence of the indenter tilt.

4. Conclusion

The analytical expressions for the calculation of the cross-section of Berkovich indenter by tilted plane were derived. These expressions were applied to the calculation of projected contact area at the nanoindentation of the tilted specimen by the Berkovich indenter. The results show that tilt lower than 1 ° gives relative difference in contact areas lower than 1 %. As the Berkovich indenter is symmetrical, the tilt around *x*-axis, which lies in the plane of symmetry, causes the symmetrical influence of the contact area. The future work could be aimed on the determination of the projected contact area of the blunted indenter.

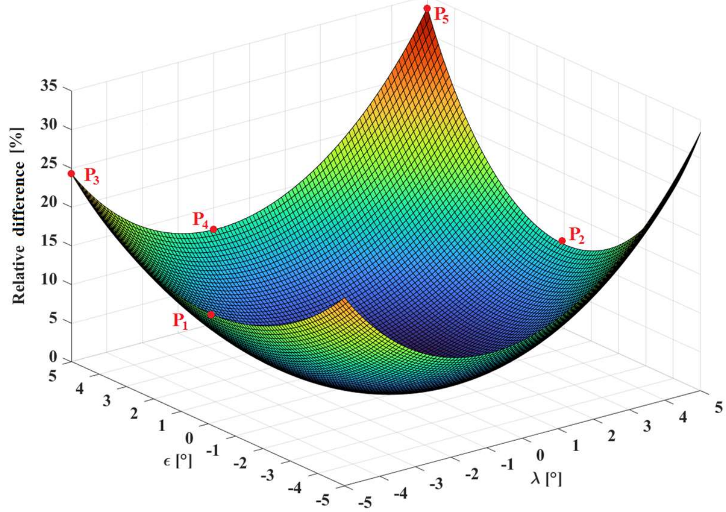

Fig. 4: Relative difference of the areas of cross-section by tilted and untilted planes at the indentation depth 100 nm (ε – tilt in x-axis, λ – tilt in y-axis).

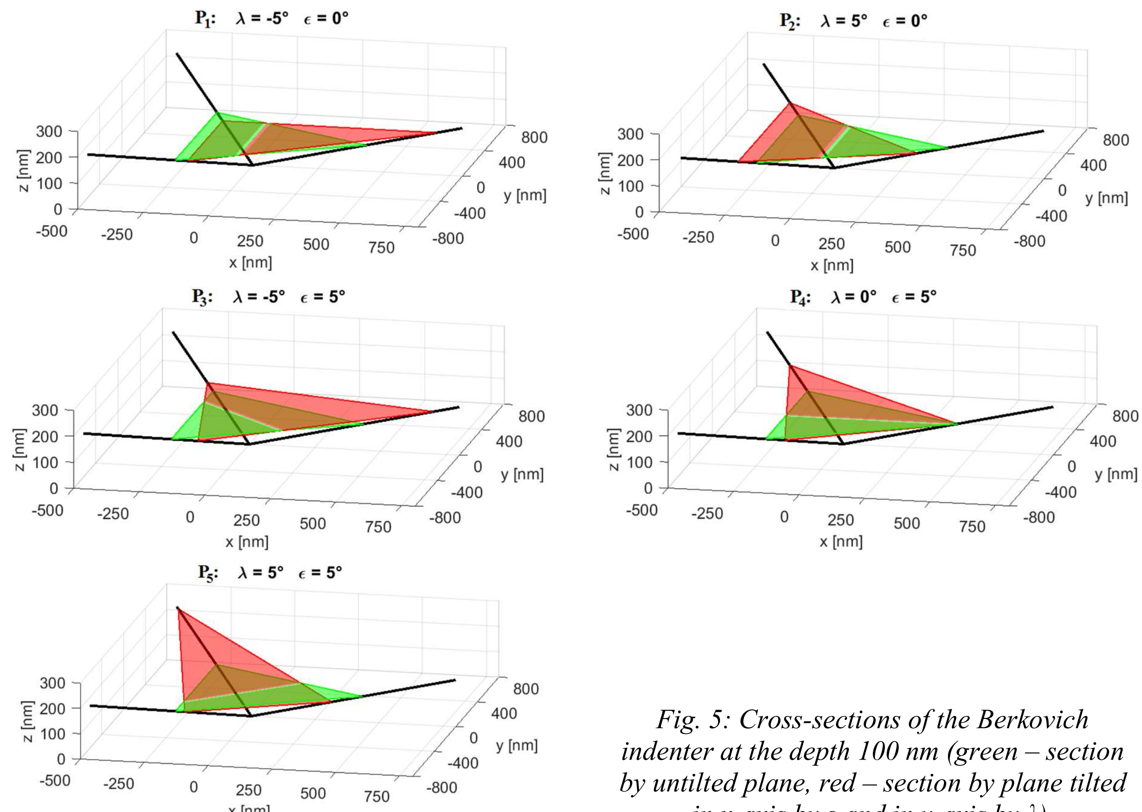

Fig. 5: Cross-sections of the Berkovich indenter at the depth 100 nm (green – section by untilted plane, red – section by plane tilted in x-axis by ε and in y-axis by λ).

Acknowledgement

This study was realized with the support by the grant FSI-S-23-8186 and with the institutional support RVO: 61388998.

References

Borodich, F. M., Keer, L. M. and Korach, C. S. (2003) Analytical study of fundamental nanoindentation test relations for indenters of non-ideal shapes. *Nanotechnology*, 14(7), 803–808.

Oliver, W. C. and Pharr, G. M. (1992) An improved technique for determining hardness and elastic modulus using load and displacement sensing indentation experiments. *Journal of Materials Research*, 7(06), 1564–1583.

Shi, C. et al. (2013) Effects of indenter tilt on nanoindentation results of fused silica: an investigation by finite element analysis. *Materials Transactions*, 54(6), 958–963.